Int. J. Heat Mass Transfer. Vol. 27, No. 8, pp. 1357–1364, 1984
Printed in Great Britain

0017-9310/84 $3.00 + 0.00

THE RADIATION SPECTRUM FROM A TEST FURNACE

D. KARMAN and F. R. STEWARD
Department of Chemical Engineering, University of New Brunswick, P.O. Box 4400, Fredericton, N.B., Canada E3B 5A3

(*Received* 14 *June* 1983 *and in revised form* 9 *November* 1983)

Abstract—The spectral distribution of radiant intensity from a test furnace (16.5 kW) was investigated experimentally and theoretically. The observed spectra were compared with model calculations based on temperature and concentration profile data. Carbon particles in the 1–10 μm diameter range were added to the propane–propylene fuel to investigate the effect of particulates. Up to a 30% increase in integrated intensity was observed at one position in the flame by adding carbon particles at a rate of 7% by weight of the fuel. Significant agglomeration of the added carbon particles takes place in the flame causing the effective concentration of small particles to be less than suggested by this addition rate. Model calculations were used to quantify this effect.

NOMENCLATURE

A_n, A_i area of nozzle and cross-sectional area of furnace excluding the nozzle, respectively [cm^2]
C'_p concentration of added carbon particles [g cm^{-3}]
Ct Craya–Curtet number, defined by equation (1)
D furnace diameter [cm]
D_p, D_{p_i} diameter of particles and the ith size fraction of added carbon particles, respectively
F dimensionless fraction defined by equation (3)
I monochromatic radiant intensity [W cm^{-2} μm^{-1} sr^{-1}]
$I(N)$ monochromatic radiant intensity emerging through Nth homogeneous region [W cm^{-2} μm^{-1} sr^{-1}]
$I(0)$ monochromatic radiant intensity leaving the confining surface for the first homogeneous region [W cm^{-2} μm^{-1}sr^{-1}]
$I_b(i)$ blackbody intensity corresponding to the temperature in the ith homogeneous region [W cm^{-2} μm^{-1} sr^{-1}]
k_a absorption coefficient [cm^{-1}]
m_n, m_i mass flow of nozzle fluid and secondary air, respectively [g s^{-1}]
n complex refractive index, $n_1 - i\,n_2$
r radial distance from furnace axis [cm]
R furnace radius [cm]
$\bar{V}$ volume fraction of soot particles in combustion chamber
w_i weight fraction of particles characterized by D_{p_i}
x axial distance along furnace from the firing end [cm]
X optical depth [dimensionless]
$X(n)$ optical depth through n homogeneous regions [dimensionless]
X_{cj} collision broadened optical depth of the jth gas [dimensionless]
$X_{particulates}$ optical depth of particulates in the ith homogeneous region [dimensionless].

Greek symbols
λ wavelength [cm]
ρ_n, ρ_i, ρ_p density of nozzle fluid, secondary air, and solid particles, respectively [g cm^{-1}]
τ transmissivity
$\tau(n)$ transmissivity through n homogeneous regions
χ_a absorption efficiency [dimensionless]
χ_{a_i} absorption efficiency of the carbon particles characterized by D_{p_i} [dimensionless].

INTRODUCTION

STUDIES of the spectral distribution of radiative transfer in furnace enclosures are relatively few owing to the difficulty of analyzing hemispherical flux from this viewpoint. The problem becomes manageable when interest is limited to the directional intensity along a line of sight through the furnace enclosure [1–3]. The interest in the study presented here comes from earlier experimental and theoretical work on the effect of solid particles on radiant transmission in furnace enclosures. Working with Al_2O_3 and MgO particles of 20 μm diameter, Steward and Gürüz [4] found that at concentrations up to 24 g m^{-3} the presence of the particulate matter did not significantly affect the total heat flux measured at the sink walls. The situation was expected to be very different when the particles have strong absorption properties and smaller sizes. A spectral analysis is desirable for investigating the qualitative as well as the quantitative effects of particulates on the emission from gaseous combustion products. The study on the strongly scattering alumina and magnesia particles was concerned with situations similar to those in metallurgical furnaces. Carbon particles on the other hand are more relevant in power generating furnaces. In particular, the addition of particulate material to natural and/or 'low BTU' gas

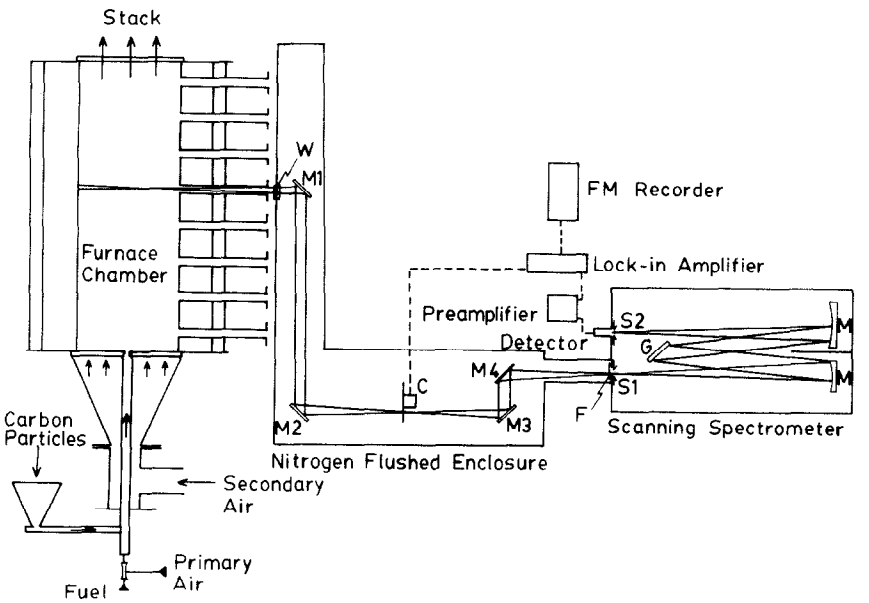

FIG. 1. Experimental apparatus.

flames with a lower emissivity than fuel oil flames is an application where the present study has direct relevance.

EXPERIMENTAL

The test furnace used in this study has been used previously for studying combustion and convective and total radiant heat transfer. Figure 1 shows a schematic diagram of the apparatus. The furnace is fully described in earlier publications [4, 5]. Gaseous fuel (50% propane, 50% propylene) and primary air are fired through ASME Standard nozzles. Secondary air enters through a porous plate covering the entire cross-section of the furnace at the bottom and combustion gases leave through a similar plate at the top. Particulate material can be introduced into the fuel plus primary air stream by a calibrated screw feeder. The combustion chamber is surrounded by a cooling jacket and is accessible to instrumentation through eight observation ports.

The long observation ports were designed for the earlier studies with the furnace and in fact present an important aperture limitation for the optics. However, they have a beneficial role in obtaining data from runs where there is particulate addition or significant indigenous soot. At the lower axial positions the pressure in the furnace is slightly below ambient and the air that fills the length of the port acts as a buffer between the window (W) and any particulate material that would otherwise accumulate on it. Any marginal absorption by the air is accounted for in the calibration procedure. At the higher ports however the furnace pressure is slightly above ambient and the ports are filled with combustion gases at low temperature. This results in re-absorption of the radiant emission from the furnace that cannot be accounted for easily. The data presented here is therefore limited to axial positions with $(x/D) < 1.6$.

Table 1 summarizes furnace dimensions and operating conditions. The Craya–Curtet number Ct is defined as [5]

$$Ct = \frac{1 + m_i/m_n}{\left[\left(\frac{\rho_i A_i}{\rho_n A_n}\right) - \left(\frac{m_i}{m_n}\right) - \frac{1}{2}\right]^{1/2}}, \quad (1)$$

and is a measure of the mixing/recirculation phenomena in the chamber. Although this study does not focus on such phenomena the Craya–Curtet number is used throughout to characterize the two sets of operating conditions. The condition $Ct = 0.18$ had earlier been extensively used [4, 5] and the resulting temperature, concentration and velocity profiles determined. The condition $Ct = 0.20$ was used during this study to reduce the contribution of indigenous soot to the radiant emission from the flame.

Concentration profiles for the gaseous species presented in Fig. 2 were measured with a Fisher gas partitioner using a water cooled probe to obtain the gas

Table 1. Furnace dimensions and operating conditions

	Diameter: 254 mm	Axial length: 724 mm
Operating conditions:		
Firing rate, kW m^{-2}	24	24
Nozzle diameter, mm	3.2	4.8
Fuel flow, kg h^{-1}	1.1	1.1
Excess air, %	20	20
Primary air, kg h^{-1}	0.65	1.21
% of total	3.0	5.5
Secondary air, kg h^{-1}	21.55	21.00
Craya–Curtet number, Ct	0.18	0.20

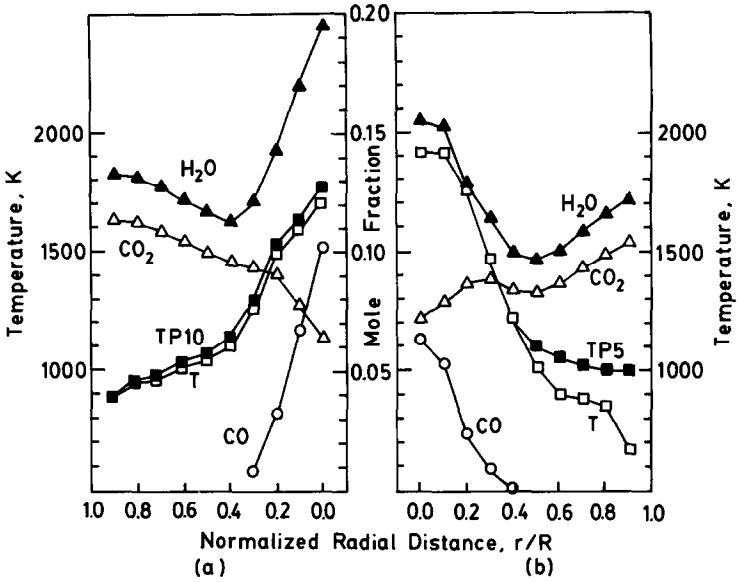

FIG. 2. Radial profiles of temperature and concentration of emitting gases: (a) $Ct = 0.18$, $x/D = 1.6$; (b) $Ct = 0.20$, $x/D = 1.6$.

samples. Temperature data for the condition $Ct = 0.18$ were obtained with a bare Pt–Pt/13%Rh thermocouple and corrected for radiation loss. The temperature data for the condition $Ct = 0.20$ were taken from a suction pyrometer with the same type of thermocouple.

The optics in Fig. 1 are mostly self-explanatory. The set of four toroidal mirrors (M1, M2, M3, M4) in the nitrogen flushed enclosure focus the beam onto the entrance slit (S1) of the spectrometer. M1 can travel parallel to the furnace axis to make observations at different ports. As the resolution of the 0.75 m Czerny–Turner spectrometer was more than adequate for this study 2000 μm slits (S1, S2) were used to provide maximum signal but minimum resolution. Three gratings (G) and five order sorting filters (F) were used in combination to cover the 1.75–10.0 μm wavelength region. The output of the thermocouple detector passes through a preamplifier followed by a lock-in amplifier working synchronously with a 13 Hz chopper (C). The analog output of the lock-in amplifier was recorded on tape and later digitized for processing.

Calibration of the spectroscopic system was done with a blackbody furnace and a Globar lamp. The Globar lamp was first calibrated against the blackbody furnace and then used as a secondary calibration source by placing it along the centerline of the furnace before a run. The digital processing of the data involved comparing the signal obtained from the combustion gases to that from the Globar lamp at 0.01 μm wavelength intervals. The monochromatic intensity thus calculated was plotted and integrated against wavelength to produce Figs. 3–6.

Spectral intensity

The spectra observed at different axial positions along the furnace are presented in Figs. 3 and 4. Most of the emission is due to the known bands of CO_2, H_2O and CO but there is also a significant continuous emission. The continuous emission is more significant at higher axial positions and for the $Ct = 0.18$ operating conditions. At the lower axial positions the emission due to the C–H bond of the fuel molecules is just noticeable in the 3–4 μm range. The integrated intensities increase along the furnace axis and are higher for the $Ct = 0.18$ conditions in this part of the furnace.

The 4.3 μm band of CO_2 changes in shape for different axial positions. This is the result of colder, CO_2 rich gas near the combustion chamber wall re-absorbing some of the emission from the combustion region. It has been demonstrated in the comparison of model calculations with experimental data that this effect, in contrast to the re-absorption within the ports, can be accounted for quantitatively since

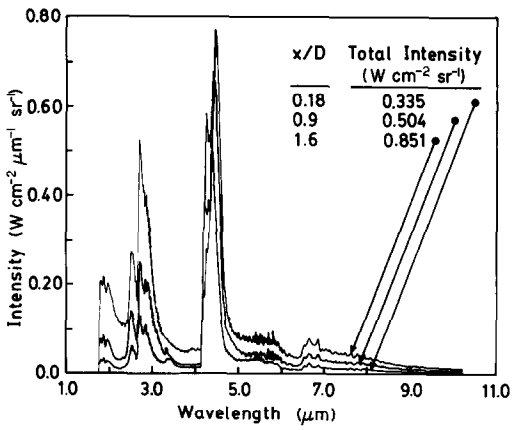

FIG. 3. Spectra observed at different axial positions for operating conditions characterized by $Ct = 0.18$.

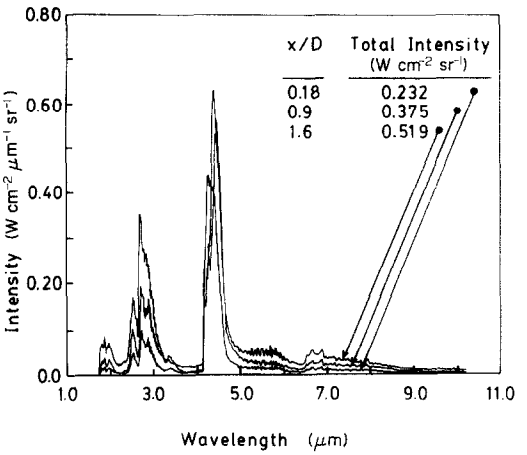

FIG. 4. Spectra observed at different axial positions for operating conditions characterized by $Ct = 0.20$.

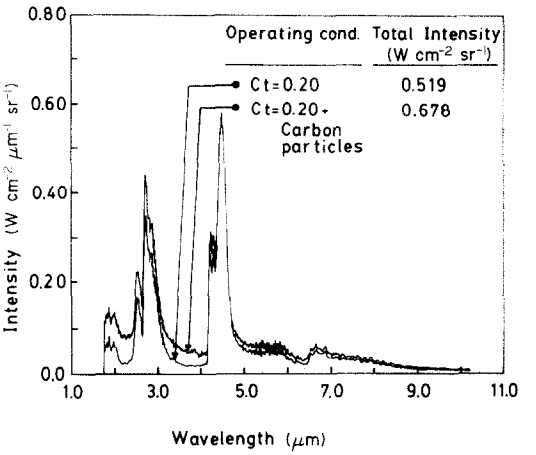

FIG. 5. Effect of carbon particle addition on the spectrum observed at $x/D = 1.6$ for $Ct = 0.18$.

the temperature and concentration profiles in the combustion chamber are available.

The condition $Ct = 0.20$ was used to reduce the contribution from indigenous soot observed for the $Ct = 0.18$ condition. This reduced, but did not entirely eliminate, the continuous emission from the propane–propylene flame.

Effect of carbon particles

Carbon particles with the size distribution given in Table 2 were introduced into the (fuel + primary air) line at a rate of 73 g h^{-1} (7% by weight of the fuel). The effect on the spectra observed at $(x/D) = 1.6$ for the two sets of operating conditions are presented in Figs. 5 and 6. Compared to the gaseous fuel only cases there is an increase in observed intensity throughout the spectrum but more significantly in the window regions between 2–3 μm and 3–4 μm. The increase in total intensity is 30% for the $Ct = 0.20$ condition and 17% for the $Ct = 0.18$ condition. Carbon particle addition at lower rates results in smaller increases. Lower flow rates however were difficult to maintain uniformly with the screw feeder and were not reliable for quantitative comparisons.

The average concentration of added carbon particles in the combustion chamber can be calculated from the input rates of fuel and carbon particles along with temperature data for the combustion chamber. However, the concentration of carbon particles in the original 1–10 μm size range is significantly less than indicated by such a calculation due to agglomeration of some of the particles. Microscopic examination of particulate material collected on a filter using a gas sampling probe shows two distinct populations:

(1) particles with a diameter less than 10 μm which represent the original size distributions;
(2) agglomerates of 150–200 μm gross dimension.

Furthermore, there are no particles of intermediate size. Tests under no-flame conditions reveal that the agglomeration is not related to the feeding mechanism but the presence of the flame. Thus, the net effect of the agglomeration is to reduce the quantity of material in the original size range while creating a few relatively large size agglomerates. The comparison of model calculations with experimental data below quantify this effect.

Table 2. Size distribution for carbon particles

Diameter (μm)	wt % less than given diameter
1	12
2	40
4	87
5	95
6.4	98
8	99
10	99.9

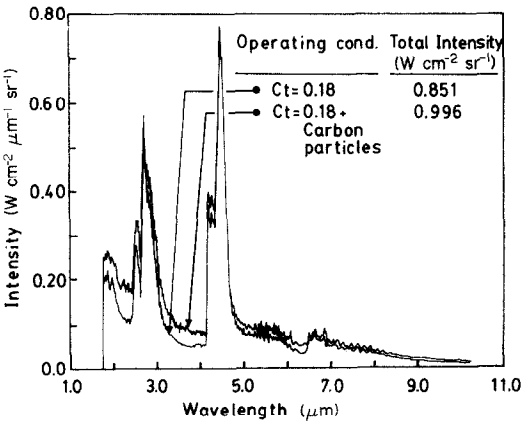

FIG. 6. Effect of carbon particle addition on the spectrum observed at $x/D = 1.6$ for $Ct = 0.20$.

THEORETICAL

The infrared activity of gaseous species arise from transitions between vibrational–rotational energy levels of the molecules, and has been treated in detail in a number of monographs [6, 7]. Band models have been generally used to represent the spectral characteristics of molecular spectra [8]. For inhomogeneous gases the Curtis–Godson approximation has been used to represent the pathlength in terms of an equivalent homogeneous pathlength. The handbook by Malkmus *et al.* [9] presents a concise overview of the concepts and contains numerous references to original sources. Grosshandler [10] presents a general purpose computer code (RADCALC) based on these techniques enabling the calculation of the monochromatic intensity emerging from an inhomogeneous path. This program was used in this study to account for the emission from the gaseous species. The experimental results of this study are compared with those of Grosshandler in a later section. The two species of particulate matter, the indigenous soot and the added carbon particles, have been treated separately in this study and the details of this procedure are presented below.

Indigenous soot

The size of soot particles generated during combustion were typically much smaller than the wavelengths of interest in radiative transfer, $(\pi D_p/\lambda) \ll 1$. Under these conditions the absorption coefficients of a cloud of soot particles is proportional to the volume fraction $\tilde{V}$ occupied by the soot particles and is given by

$$k_a = \frac{36\pi \tilde{V} F}{\lambda}, \tag{2}$$

where F is a function of the complex refractive index of the soot

$$F = \frac{n_1 n_2}{(n_1^2 - n_2^2 + 2)^2 + (2n_1 n_2)^2}. \tag{3}$$

The absorption coefficient is therefore dependent on wavelength both through the wavelength dependency of the complex refractive index as well as the strong $1/\lambda$ dependency in equation (2). The complex refractive index of soot is very much influenced by the source material and the combustion conditions under which it is generated. The dispersion equations describing the wavelength dependency of n_1 and n_2 for propane soot with a H/C ratio of 1/4.6 reported by Dalzell and Sarofim [11] were used to calculate the absorption coefficient. This gave good representation of the emission from soot found in this study.

Carbon particles of 1–10 *μm diameter*

For particulate matter of size comparable to the wavelength of radiant emission, the rigorous solution of Maxwell's equations must be used to calculate the extinction and scatter efficiencies as well as the angular distribution for scattered radiation. This solution is given by Hottel and Sarofim [12]. A computer code based on these equations and written by Gürüz [13] was used to calculate absorption efficiencies, χ_a, given the complex refractive index and the size parameter $\pi D_p/\lambda$. These calculations are also dependent on wavelength through the wavelength dependency of the complex refractive index and the size parameter. Of these, the size parameter has by far the more significant influence. Due to the complexity of the calculations for each pair of size parameter and complex refractive index, the wavelength dependency of the latter was neglected and a constant value of $n = 2.29 - 1.49$ i recommended by Gürüz used. The absorption coefficient of the cloud of particles with the size distribution given in Table 2 was calculated by adding the contributions from the different size fractions. The cumulative effect of seven size fractions is therefore given by

$$k_a = \frac{3}{2}\frac{C'_p}{\rho_p}\sum_{i=1}^{7}\frac{w_i}{D_{p_i}}\chi_{a_i}. \tag{4}$$

Calculation sequence

Given the absorptive properties of the gases and the particulates the optical depth X through N homogeneous regions is found by

$$X(N) = \sum_{j=1}^{3} X_{c_j}(N) + \sum_{i=1}^{N} (X_{\text{particulates}})_i, \tag{5}$$

where the first summation is over the number of active gaseous species while the second summation over N regions incorporates the two types of particulate material as well as the different size fractions for the larger carbon particles. The transmissivity τ, through N regions is defined by

$$\tau(N) = \exp(-X(N)), \tag{6}$$

hence the intensity I, emerging through the Nth region is given by

$$I(N) = I(0)\tau(N) + \sum_{i=1}^{N} I_b(i)[\tau(N) - \tau(N-1)], \tag{7}$$

which is the integrated form of the equation of transfer for discrete intervals. Temperature and concentration data from 23 regions of 6–19 mm represent the entire inhomogeneous path of 254 mm. The monochromatic intensity calculation is carried out 127 times to cover the 1.75–10.0 μm wavelength region at wavenumber intervals of 20–100 cm^{-1} depending on the region of the spectrum.

COMPARISONS

The model calculations based on measured species' concentration and temperature profiles are compared with the observed spectra in Figs. 7–10. In Figs. 7 and 9 the model calculations designated 'measured profiles' do not include the effect of indigenous soot and use temperatures equivalent to the millivolt reading from the suction pyrometer. By using a uniform soot fraction

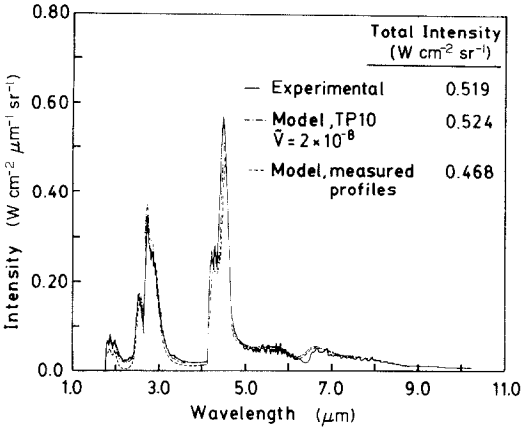

FIG. 7. Comparison of model calculations with observed spectra at $x/D = 1.6$ for $Ct = 0.20$.

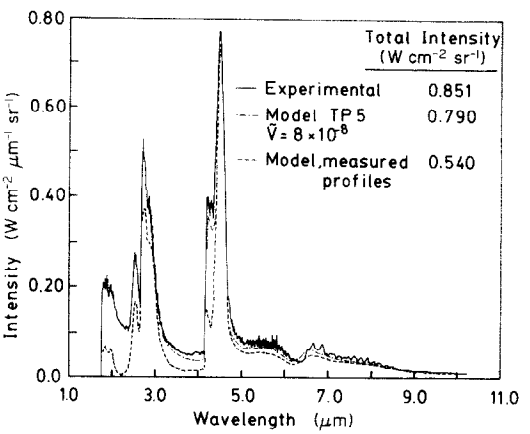

FIG. 9. Comparison of model calculations with observed spectra at $x/D = 1.6$ for $Ct = 0.18$.

$\bar{V}$ as an adjustable parameter and correcting the measured profiles for possible uncertainties, a better agreement between model calculations and observed spectra is obtained. The temperature profiles designated TP5 and TP10 in Figs. 7 and 9 can be compared with the observed profiles in Figs. 2(a) and (b) and represent positive corrections to the measured profile at the higher temperatures. Comparisons between model calculations and observed spectra are presented in Figs. 8 and 10 for runs with carbon particle addition. The observed spectra in these figures are those in Figs. 5 and 6, respectively. The model calculations are obtained by adding the effect of carbon particles to the cases in Figs. 7 and 9 which give good agreement without the carbon particle addition. The concentration of carbon particles used in these calculations is one third of that computed from the average flow rates of gas and 1–10 μm particles into the furnace. This value, although low is in general agreement with the observed agglomeration mentioned above. Considering the agglomerates to be 10 times larger than the original particles and to have an average density of one half that of the original particles, the reduction of the concentration of the small particles would require the ratio of the numbers of agglomerates to small particles to be 1 : 250. The number densities observed on filters used during sampling indeed show a ratio of this magnitude.

Figure 10 indicates that there is some qualitative disagreement between model calculations and the observed spectrum for $Ct = 0.18$ operating conditions with carbon particle addition although the no-particles-added case shows good agreement in Fig. 9. It can be expected that the carbon particle distribution for the $Ct = 0.18$ condition is different from the uniform distribution assumed for the $Ct = 0.20$ condition where the ratio of particles to nozzle fluid is less. The quantitative agreement however is comparable to

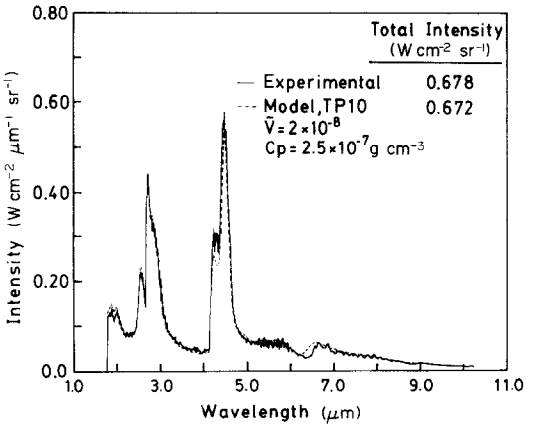

FIG. 8. Comparison of model calculations with observed spectra at $x/D = 1.6$ for $Ct = 0.20$ when 1–10 μm carbon particles are added at a rate of 7% by weight of the $C_3H_6 + C_3H_8$ fuel.

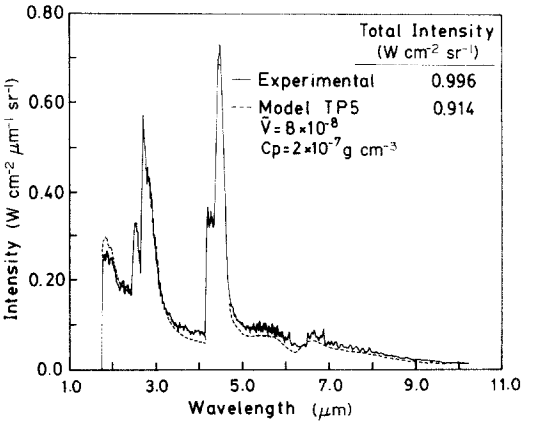

FIG. 10. Comparison of model calculations with observed spectra at $x/D = 1.6$ for $Ct = 0.18$ when 1–10 μm carbon particles are added at a rate of 7% by weight of the $C_3H_6 + C_3H_8$ fuel.

previous cases and, given the nature of these comparisons, does not merit further speculation.

DISCUSSION AND CONCLUSIONS

The experimental results of the study indicate that the radiant emission from a flame is significantly increased by the addition of small quantities of strongly absorbing/emitting particles in the 1–10 μm diameter size range even when the original flame already has a significant contribution from indigenous soot. It can be expected that the increase would be larger in the case of a flame without significant soot such as a natural gas flame.

The spectral distribution of the emission from the flame can be interpreted rigorously, using available models for the radiative properties of the contributing species and temperature–concentration data. The radiative properties of 1–10 μm diameter carbon particles calculated from the Mie equations were satisfactory for interpreting experimental results insofar as the spectral distribution of radiation was concerned. The uncertainty in the concentration of the particles, however, masks any discrepancy in total intensity that may be attributed to the computed radiative properties.

It is worthwhile to point out one difference between the present study and Grosshandler's work with methanol and a methanol–coal slurry [2]. In the latter, the addition of coal particles to the liquid fuel also required changing the fuel nozzle so that temperature and concentration profiles were different from those with methanol alone. The comparisons between the two types of fuel therefore indicate the combined effect of adding the coal and changing nozzles. In the present study, carbon particle addition did not pose any operational problems hence direct comparison between gaseous fuel and gaseous fuel + carbon particles cases was possible. The general conclusions however are in agreement and the calculations in the present study point to the utility of Grosshandler's RADCALC with only minor modifications.

REFERENCES

1. R. Echigo, N. Nishiwaki and M. Hirata, A study on the radiation of luminous flames, *Proc. 11th Symp. (Int.) on Combustion*, pp. 381–389. Combustion Institute (1966).
2. W. L. Grosshandler, Radiation from a methanol furnace, *Trans. Am. Soc. Mech. Engrs*, Series C, *J. Heat Transfer* **100**, 247–252 (1978).
3. T. Sato, T. Kunimoto, S. Yoshii and T. Hashimoto, On the monochromatic distribution of the radiation from the luminous flame, *Bull. J.S.M.E.* **12**, 1135–1143 (1969).
4. F. R. Steward and K. H. Gürüz, The effect of solid particles on radiative transfer in a cylindrical test furnace, *Proc. 15th Symp. (Int.) on Combustion*, pp. 1271–1283 (1974).
5. F. R. Steward, S. Osuwan and J. J. C. Picot, Heat transfer measurements in a cylindrical test furnace, *Proc. 14th Symp. (Int.) on Combustion*, pp. 651–660 (1972).
6. S. S. Penner, *Quantitative Molecular Spectroscopy and Gas Emissivities*. Addison-Wesley, Reading, Massachusetts (1959).
7. G. Herzberg, *Molecular Spectra and Molecular Structure*. Van Nostrand, Princeton, New Jersey (1950).
8. G. N. Plass, Models for spectral band absorption, *J. Opt. Soc. Am.* **48**, 690–703 (1958).
9. W. Malkmus, C. B. Ludwig, J. E. Reardon and J. A. D. Thomson, *Handbook of Infrared Radiation from Combustion Gases*, NASA SP-3080 (1973).
10. W. L. Grosshandler, A study of a model furnace burning methanol and a methanol/coal slurry, Ph.D. thesis, University of California, Berkeley, California (1976).
11. W. H. Dalzell and A. F. Sarofim, Optical constants of soot and their application to heat-flux calculations, *Trans. Am. Soc. Mech. Engrs*, Series C, *J. Heat Transfer* **91**, 100–104 (1969).
12. H. C. Hottel and A. F. Sarofim, *Radiative Transfer*. McGraw-Hill, New York (1967).
13. K. H. Gürüz, The effect of solid particles on radiant transmission in furnace enclosures, Ph.D. thesis, University of New Brunswick, Fredericton, New Brunswick (1973).

LE SPECTRE DE RAYONNEMENT D'UN FOUR EXPÉRIMENTAL

Résumé—La distribution spectrale d'intensité de rayonnement d'un four expérimental (16.5 kW) est étudiée expérimentalement et théoriquement. Les valeurs expérimentales sont comparées avec les valeurs théoriques basées sur les mesures des profils de température et concentration. On a ajouté des particules de carbone de grandeur entre 1 et 10 μm au combustible (un mélange de propane et de propylène). On a constaté au augmentation de 30% de l'intensité intégrale dans une position de la flamme pour un taux d'addition de 7% de particules par rapport au débit de masse du gaz combustible. On a remarqué une agglomération des particules dans la flamme, ce qui provoque une chute de la concentration effective de particules. L'effet de cette chute est étudié d'après le modèle théorique.

DAS STRAHLUNGSSPEKTRUM EINES TESTOFENS

Zusammenfassung—Es wurde die spektrale Verteilung der Strahlungsintensität eines Testofens (16,5 kW) experimentell und theoretisch untersucht. Die beobachteten Spektren wurden mit Modellrechnungen verglichen, die auf Daten von Temperatur und Konzentrationsprofilen beruhen. Dem Propan–Propylen–Brennstoff werden Kohlenstoffpartikel von 1–10 μm Durchmesser beigemischt, um den Einfluß der Teilchen zu untersuchen. Dabei wurde durch Hinzufügen von Kohlenstoffteilchen im Verhältnis von 7% des Brennstoffgewichts eine 30% ige Zunahme der integralen Intensität an einer Stelle der Flamme beobachtet. Es tritt eine beachtliche Agglomeration der zugesetzten Kohlenstoffteilchen in der Flamme auf, wodurch die effektive Konzentration der Partikel niedriger wird, als entsprechend der zugesetzten Menge zu erwarten wäre. Durch Modellrechnungen konnte dieser Effekt quantitativ beschrieben werden.

СПЕКТР ИЗЛУЧЕНИЯ ЛАБОРАТОРНОЙ ПЕЧИ

Аннотация—Экспериментально и теоретически исследуется спектральное распределение интенсивности излучения лабораторной печи (16,5 кВт). Экспериментально наблюдаемые спектры сравниваются с результатами модельных расчетов, основанных на данных о распределениях температуры и концентрации. Для выяснения влияния микрочастиц на излучение в пропано-пропиленовое топливо добавлялись частицы угля с диаметрами от 1 до 10 мкм. В одном выбранном для измерения месте в пламени наблюдалось примерно 30% увеличение интенсивности излучения при вводе частиц угля, составлявших 7% от веса топлива. В пламени происходит заметная агломерация угольных частиц, в результате чего значение эффективной концентрации мелких частиц оказывается меньшим, чем рассчитанное при 7% подаче. Для количественного объяснения этого эффекта использовались модельные расчеты.